Received: 4 December 2022 | Accepted: 9 May 2023

DOI: 10.1111/1462-2920.16426

RESEARCH ARTICLE

ENVIRONMENTAL MICROBIOLOGY Applied Microbiology International

Cell surface composition, released polysaccharides, and ionic strength mediate fast sedimentation in the cyanobacterium *Synechococcus elongatus* PCC 7942

Julie A. Z. Zedler[1] | **Marlene Michel**[2] | **Georg Pohnert**[2] | **David A. Russo**[2]

[1]Friedrich Schiller University Jena, Matthias Schleiden Institute for Genetics, Bioinformatics and Molecular Botany, Synthetic Biology of Photosynthetic Organisms, Jena, Germany

[2]Friedrich Schiller University Jena, Institute for Inorganic and Analytical Chemistry, Bioorganic Analytics, Jena, Germany

Correspondence
David A. Russo, Friedrich Schiller University Jena, Institute for Inorganic and Analytical Chemistry, Bioorganic Analytics, Lessingstr. 8, D-07743 Jena, Germany.
Email: david.russo@uni-jena.de

Funding information
Alexander von Humboldt-Stiftung; Deutsche Forschungsgemeinschaft, Grant/Award Numbers: EXC 2051—Project-ID 390713860, SFB 1127 ChemBioSys project number, 239748522

Abstract

Cyanobacteria are photosynthetic prokaryotes of high ecological and biotechnological relevance that have been cultivated in laboratories around the world for more than 70 years. Prolonged laboratory culturing has led to multiple microevolutionary events and the appearance of a large number of 'domesticated' substrains among model cyanobacteria. Despite its widespread occurrence, strain domestication is still largely ignored. In this work we describe *Synechococcus elongatus* PCC 7942-KU, a novel domesticated substrain of the model cyanobacterium *S. elongatus* PCC 7942, which presents a fast-sedimenting phenotype. Under higher ionic strengths the sedimentation rate increased leading to complete sedimentation in just 12 h. Through whole genome sequencing and gene deletion, we demonstrated that the Group 3 alternative sigma factor F plays a key role in cell sedimentation. Further analysis showed that significant changes in cell surface structures and a three-fold increase in released polysaccharides lead to the appearance of a fast-sedimenting phenotype. This work sheds light on the determinants of the planktonic to benthic transitions and provides genetic targets to generate fast-sedimenting strains that could unlock cost-effective cyanobacterial harvesting at scale.

INTRODUCTION

Every axenic laboratory culture ultimately derives from a 'wild' environmental ancestor. The transition from the environment to the laboratory typically implies moving from a highly fluctuating, competitive environment to a single species, static culture. The adaptation of environmental isolates to their laboratory habitat is termed domestication (Eydallin et al., 2014). Virtually all modern model organisms have undergone decades of domestication and cyanobacteria, globally important phototrophic prokaryotes, are not an exception. Due to the interest in their ecology, physiology, and, more recently, biotechnological applications, cyanobacterial model strains have been maintained in laboratories around the world for more than 70 years (Bryant, 2014). The continuous culturing, passaging, and mutation of cyanobacterial strains has led to domestication and the concomitant appearance of multiple substrains. The extent of which was first highlighted in the widely used *Synechocystis* sp. PCC 6803 (hereafter *Synechocystis*) (Trautmann et al., 2012). *Synechocystis* was originally isolated in 1968 and soon after diverged into two lineages, PCC 6803 and ATCC 27184 (Ikeuchi & Tabata, 2001). From the latter, glucose-tolerant substrains emerged (Williams, 1988) and rapidly became popular hosts due to the availability of a sequenced genome (Kaneko et al., 1996) and their ease of cultivation (e.g., growth on glucose, lack of motility and aggregation). On the other hand, strains of the PCC 6803 lineage have played a

key role in unravelling the mechanisms behind motility, phototaxis, and protein secretion (Bhaya et al., 1999; Russo et al., 2022; Schuergers et al., 2016).

A similar pattern of laboratory domestication is now emerging for another well-studied freshwater cyanobacterium, *Synechococcus elongatus* (hereafter *S. elongatus*) (Adomako et al., 2022). *S. elongatus* PCC 7942 has been used extensively as a model for the prokaryotic circadian clock (Cohen & Golden, 2015). Recently, it has also been used to study natural competence (Schirmacher et al., 2020; Taton et al., 2020) and developed as a biotechnological chassis (Santos-Merino et al., 2019). The origin of *S. elongatus* can be tracked back to early isolations in Waller Creek, Texas and later in San Francisco, California (Golden, 2019; Stanier et al., 1971). Several *S. elongatus* strains were isolated and deposited in the Pasteur Culture Collection, however only PCC 6301 (alias UTEX 625) and PCC 7942 were widely adopted. In 2015, a fast-growing strain of *S. elongatus*, UTEX 2973, was isolated from a frozen archive of UTEX 625 (Yu et al., 2015). While the exact origin of UTEX 2973 remains a mystery, it is likely that the specific growth conditions used in this laboratory (e.g., high light and high CO_2) might have favoured the appearance of a fast-growing substrain. Another addition to the *S. elongatus* group of substrains was UTEX 3055, an environmental isolate from Waller Creek whose genome shares a 98.5% identity with that of PCC 7942 (Yang et al., 2018).

Further evidence for laboratory domestication arises from the distinct phenotypes presented by the *S. elongatus* substrains. For example, the laboratory strains PCC 6301, PCC 7942, and UTEX 2973 share a genome identity of 99.99%. However, when compared to PCC 7942, both PCC 6301 and UTEX 2973 lack natural competence, and the ability to take up and incorporate foreign DNA (Schirmacher et al., 2020; Taton et al., 2020). It has been suggested that this is due to the presence of single nucleotide polymorphisms (SNPs) in critical subunits of the type IVa pili system (T4aPS) (Li et al., 2018). UTEX 2973 also exhibits a fast-growing and high-light tolerant phenotype (Ungerer, Lin, et al., 2018; Ungerer, Wendt, et al., 2018). A more dramatic phenotypical difference can be seen in the environmental isolate UTEX 3055. In laboratory conditions, UTEX 3055 forms biofilms and is capable of phototactic motility with a unique bidirectional photoreceptor (Yang et al., 2018). PCC 7942 is not phototactic, however, the genes encoding for this photoreceptor, and other components of the phototaxis pathway, are present in its genome. In addition, PCC 7942 does not form biofilms, however, mutations in key T4aPS components (e.g., PilB1) lead to a strong biofilm-forming phenotype (Schatz et al., 2013). Therefore, it has been suggested that phototactic motility and biofilm formation are intrinsic properties of *S. elongatus* and were lost during laboratory domestication (Adomako et al., 2022). Interestingly, genotype-to-phenotype analyses of domesticated *Synechocystis* and *S. elongatus* strains indicate similar loss-of-function patterns. These include extensively modified cell surfaces (e.g., loss of pili and changes in polysaccharide composition) and loss of environmentally relevant behaviours such as motility, phototaxis, and biofilm formation. Despite ample evidence of substrain individuality, *Synechocystis* and *S. elongatus* substrains are widely used and strain domestication has received little attention.

In this study we describe a new *S. elongatus* substrain, PCC 7942-KU (hereafter 7942-KU), that shows a fast-sedimenting phenotype. We demonstrate that fast sedimentation occurs due to changes in cell surface composition mediated, in part, by a mutation in the Group 3 sigma factor, SigF. Our findings present a unique opportunity to investigate the mechanisms that underly the switch from a planktonic to a benthic state. In addition, fast sedimentation also enables efficient and low-cost harvesting for cyanobacterial bioproduction.

EXPERIMENTAL PROCEDURES

Strains and growth conditions

In this study two strains of *S. elongatus* were used: *S. elongatus* PCC 7942 (obtained from the Pasteur Culture Collection of Cyanobacteria), here referred to as 7942-WT, and *S. elongatus* PCC 7942-KU (named after its place of origin, Københavns Universitet and kindly donated by Yumiko Sakuragi). 7942-KU has been deposited in the DSMZ strain collection under accession no. DSM 115314. Cultures were maintained on BG-11 medium (Stanier et al., 1971) supplemented with 10 mM 2-*tris*(hydroxymethyl)-methyl-2-amino 1-ethanesulfonic acid (TES) buffer (pH 8.0) and 1.5% (*w*/*v*) Kobe I agar at 30°C with continuous illumination of approximately 25 μmol photons m^{-1} s^{-1}. To prevent genetic drift, cultures were taken out of their respective cryo archives at least every 3 weeks. Liquid cultures were grown either in BG-11 TES medium or P4-TES CPH medium (Russo et al., 2019), a modified version of phosphate-replete medium (Lippi et al., 2018). Experiments in liquid culture were performed either in 100 mL flasks, T-25 cell culture flasks, 48-well flat-bottom microplates, or a CellDEG high-density system (HDC 6.10 starter kit; CellDEG). The CellDEG system was set up as previously described (Cao et al., 2022). All liquid cultures were illuminated by Lumilux cool white L 15 W/840 fluorescent lamps (Osram), with continuous illumination of approximately 50 μmol photons m^{-2} s^{-1}, and shaken at 150 rpm (flasks, microplates) or 280 rpm (CellDEG) on a Unimax 1010 orbital shaker (Heidolph Instruments). For cultivation of the 7942-WT mutants, agar plates were supplemented with 25 μg mL^{-1} kanamycin (7942-WT Δ*pilB1*, 7942-KU + *sigF*) or 5 μg mL^{-1} gentamycin (7942-WT Δ*sigF*, 7942-WT Δ*pilT1*). Antibiotics were not added to liquid cultures to avoid distorting effects.

Sedimentation and biofilm assays

For biofilm quantification, cultures were grown in BG-11 TES medium for 3 days in glass tubes at 30°C with constant illumination and bubbled with 3% CO_2-supplemented air. The cultures were then diluted to an $OD_{750\ nm} = 0.5$ in 20 mL and grown in the same conditions for a further 5 days. Ferric ammonium citrate and citric acid were added fresh at every culture transfer and the tip of the Pasteur pipette supplying aeration was placed 1–2 cm above the bottom of the tube. Biofilm quantification followed previously established protocols (Sendersky et al., 2017) with the exception that chlorophyll extraction and estimation was adapted from Ritchie (2008). Briefly, 1 mL of culture was centrifuged at 10,000 $\times g$ for 5 min. The supernatant was discarded, and the pellet was resuspended in 1 mL of 90% methanol. Samples were then incubated for 10 min in the dark and centrifuged at 10,000 $\times g$ for 5 min. The supernatant was measured at 665 nm and chlorophyll concentrations were estimated with the equation Chl *a* ($\mu g\ mL^{-1}$) = $A_{665\ nm} \times 12.9447$. For the sedimentation analysis in 100 mL flasks, cultures were grown for 5 days at 30°C under shaking and constant illumination. The cultures were then diluted to an $OD_{750\ nm} = 1$ in 25 mL of the respective medium, transferred to 100 mL flasks, and kept at room temperature, without agitation, under constant illumination, for approximately 14 days. For sedimentation analysis in 30 mL universal tubes and 48-well microplates, cultures were inoculated at an $OD_{750\ nm} = 0.4$ and grown for 3 days at 30°C in the CellDEG system under shaking and constant illumination. For the assay in universal tubes, cultures were then diluted to an $OD_{750} = 1.5$ in 15 mL of the respective medium and kept at room temperature, without agitation, under constant illumination, for 24–48 h. For the microplate assay, cultures were diluted to an $OD_{750\ nm} = 1.0$ in 200 μL of the respective medium and monitored with multipoint absorbance measurements (13 coordinates, $OD_{750\ nm}$) over 20 min on a Varioskan Flash microplate reader (Thermo Fisher Scientific). Microplates were kept in the reader at room temperature, without agitation or illumination during the assay. In the experiments where the addition of $MgSO_4$, Na_2SO_4, NaCl, or cAMP was tested, these components were added 2 h before the sedimentation analysis. The relative absorbance represents the ratio between the maximum value among the 13 coordinates at T_n and the mean of all 13 coordinates at T_0 (relative absorbance = max T_n/mean T_0).

Resequencing of *S. elongatus* PCC 7942-KU

For sequencing 7942-KU, genomic DNA was extracted with the Quick-DNA Fungal/Bacterial Miniprep Kit (Zymo Research Europe) following the manufacturer's recommendations with the following modifications. Cell lysis was conducted with Genomic Lysis Buffer in ZR BashingBead Lysis Tubes with a Vortex-Genie 2 (Scientific Industries) on setting 7 for 20 min. The sample was then centrifuged at 10,000 $\times g$ for 2 min and the supernatant was column purified. Elution was performed in 100 μL of DNA Elution Buffer. To remove RNA from the sample, the eluate was brought to a final volume of 200 μL with DNA Elution Buffer and 10 μL of a 10 mg mL^{-1} solution of RNase A. The sample was gently mixed and incubated at 37°C for 60 min. A final clean-up was then conducted using the same column purification protocol. Genomic DNA was eluted in 50 μL of DNA Elution Buffer and yields were measured on a Qubit fluorometer (Invitrogen). Illumina 2 × 150 bp paired-end library preparation and sequencing was performed by Eurofins Genomics using their INVIEW Resequencing service for bacterial genomes and mapped against the 7942-WT genome (GenBank accession no. NC_007604). All SNPs identified in protein-coding regions were confirmed by PCR and Sanger sequencing using the primers listed in Table S1.

Generation of *S. elongatus* PCC 7942 mutants

Constructs for the generation of mutants were assembled by Gibson assembly (Gibson et al., 2009) using NEBuilder Hifi DNA Assembly Master Mix (New England Biolabs). To generate a plasmid for the knockout of Synpcc7942_1510 (SigF), four DNA fragments were generated by PCR for plasmid assembly: a vector backbone of pBR322 without the tetracycline resistance cassette, 1000 bp genomic regions up- and downstream of Synpcc7942_1510 for homologous recombination and a gentamycin resistance cassette. The generated plasmid was named pJZ170. The plasmid for the knockout of Synpcc7942_2070 (PilT1) was generated using the same strategy with a 1000 bp region upstream and a 1025 bp region downstream of Synpcc7942_2070. The generated plasmid was termed pDAR27. A plasmid for knocking out Synpcc7942_2071 (PilB1) was generated using a vector backbone fragment generated from pCAT.015 (Vasudevan et al., 2019) (gift from Alistair McCormick, Addgene plasmid # 119558) digested with XbaI and three fragments amplified by PCR: a Kanamycin resistance cassette and 1500 bp genomic regions up- and downstream of Synpcc7942_2071 for homologous recombination. This plasmid was named pMM02. For the complementation of *sigF* in 7942-KU, the gene sequence of 7942-WT *sigF* (Synpcc7942_1510) was fused with an HA-epitope encoding sequence, and a J23100 promoter was used to control gene expression.

The sequence was flanked by genomic regions for integration into neutral site 1 on the genome (plasmid pJZ169). The correct assembly of constructs was confirmed by Sanger sequencing. The generated constructs were transformed into 7942-WT (pJZ170, pMM02, and pDAR27) or 7942-KU (pJZ169) using natural competence. Transformants were streaked on increasing concentrations of antibiotics (up to 10 μg mL^{-1} gentamycin or 50 μg mL^{-1} kanamycin) until full segregation was confirmed by colony PCR. Fully segregated mutant strains were named 7942-WT Δ*sigF* (transformed with pJZ170), 7942-WT Δ*pilT1* (transformed with pDAR27), 7942-WT Δ*pilB1* (transformed with pMM02) and 7942-KU + *sigF* (transformed with pJZ169). All primers used for generation of constructs and colony PCR are listed inTable S2.

Microbial adhesion to hydrocarbons assay

The microbial adhesion to hydrocarbons (MATH) assay was performed following the original publication (Rosenberg et al., 1980) with some modifications. Exponentially growing cyanobacterial cells were harvested and washed twice in phosphate buffer (22.2 g L^{-1} K_2HPO_4, 7.2 g L^{-1} KH_2PO_4), pH 7.1. Following this, cells were resuspended to, approximately, an $OD_{750\ nm} = 0.35$ in 1.6 mL of phosphate buffer with 2 M ammonium sulphate in glass vials. The addition of ammonium sulphate enhances hydrophobic interactions and, thus, the sensitivity of the assay (Rosenberg, 1984). To the 1.6 mL cyanobacterial suspension, 400 μL of *p*-xylene was added, the mixture was vortexed at maximum speed for 2 min and then allowed to rest for 15 min. A total of 800 μL were harvested from the aqueous phase and the $OD_{750\ nm}$ was measured. The MATH score is calculated using the equation $(1 - OD_{final}/OD_{initial}) \times 100$.

Determination of total carbohydrate content, CPS and RPS

Sample preparation for the quantification of total carbohydrates, capsular polysaccharides (CPS), and released polysaccharides (RPS) was done according to Mota et al. (2013) and Flores et al. (2019). Briefly, 10 mL of culture were transferred to ReadyLyzer 10 dialysis membranes (molecular weight cut-off 12–14 kDa, Serva) and dialyzed against 10 volumes of water for 24 h with continuous stirring. From the dialyzed samples, 5 mL were used to determine total carbohydrates, and 5 mL were centrifuged at 4000 ×*g* for 15 min. The supernatant of the latter was used for RPS determination. The resulting pellet was resuspended in 5 mL of water, incubated at 95°C for 15 min, and centrifuged at 4000 ×*g* for 15 min. The supernatant was then used for CPS determination. Total carbohydrate content, CPS, and RPS was determined using the phenol-sulfuric acid assay described in DuBois et al. (1956).

RESULTS

7942-KU exhibits a strong sedimentation phenotype in high-density medium

7942-KU was revived from an *S. elongatus* cryo archive at the University of Copenhagen. Although the complete strain history is unknown, 7942-KU has its origins in *S. elongatus* PCC 7942-AMC06. This strain is routinely used in the laboratory of Susan Golden (UC San Diego) and was donated to a European cyanobacterial research group before 2012. Given it had spent more than a decade being cultivated and transferred among European laboratories, we hypothesized that it could have undergone laboratory domestication. Therefore, we purchased *S. elongatus* PCC 7942 from the Pasteur Culture Collection (hereafter 7942-WT) and initiated a phenotypic comparison between both strains. It was immediately evident that 7942-KU exhibited a sedimenting phenotype when cultivated in the high-density medium P4 (Figure 1A). To further investigate this phenomenon, both strains were cultivated in BG-11 and P4 media and the sedimentation rates were investigated over 24 h (Figure 1B). In BG-11 medium, 7942-WT did not sediment and only minor sedimentation was observed in 7942-KU. In P4 medium, 3 h are sufficient for a large part of the 7942-KU culture to sediment. Full sedimentation was achieved after 12 h with little difference observed between 12 and 24 h. 7942-WT also exhibited a faster sedimentation rate when grown in P4 medium, however, the culture never completely sedimented during the experiment. After 24 h of static incubation, the sedimented cultures could be completely resuspended by vortexing (Figure S1).

In 7942-WT, it has been reported that mutations in key type IVa pili (T4aP) components (i.e., mutations that eliminate pili formation) lead to a strong biofilm-forming phenotype (Nagar et al., 2017; Schatz et al., 2013). Therefore, to distinguish the sedimentation phenotype from the biofilm-forming phenotype, biofilm formation was quantified in 7942-WT, 7942-KU, and a 7942-WT Δ*pilB1* (Synpcc7942_2070) mutant. PilB1 is the T4aP retraction ATPase, and its inactivation abrogates pili formation and activates a biofilm-forming phenotype (Nagar et al., 2017; Schatz et al., 2013). In 7942-WT and 7942-KU most of the chlorophyll remained in suspension (99.48% ± 0.12% and 90.83% ± 2.21%, respectively) (Figure 1C, Figure S2). However, 7942-WT Δ*pilB1* strongly adhered to the culture vessel and only 37% ± 3.40% of chlorophyll remained in suspension (Figures 1C, S2).

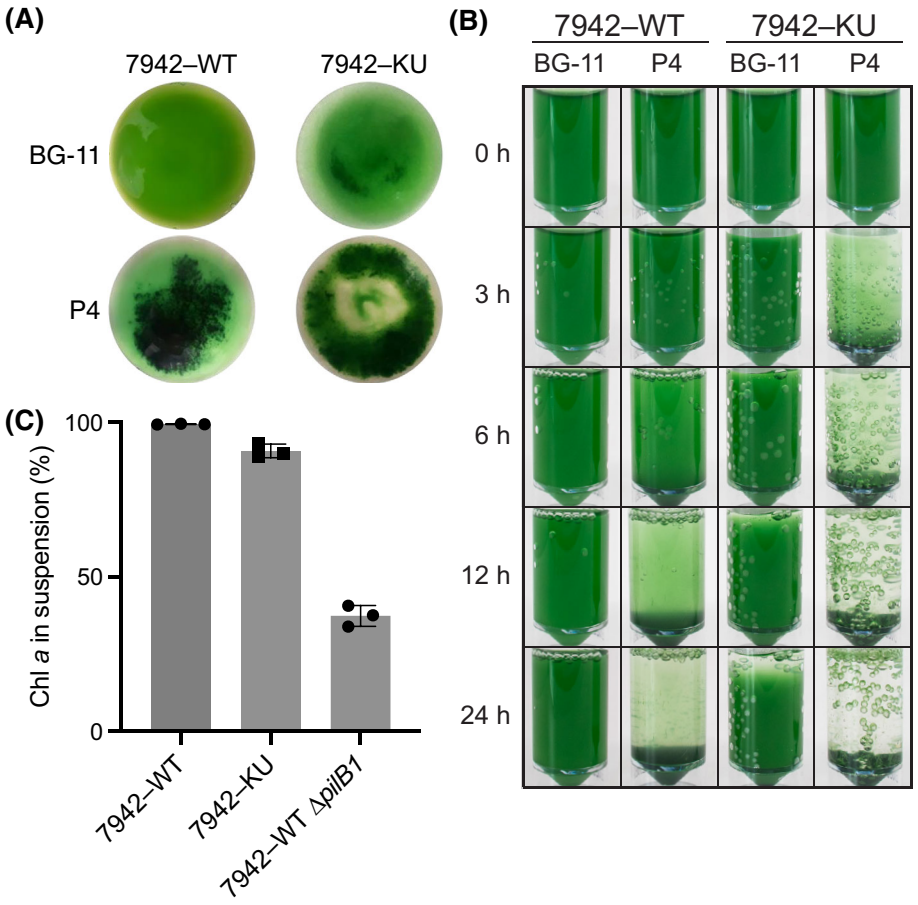

FIGURE 1 Sedimentation and biofilm formation of 7942 strains.(A) 20 mL culture of 7942-WT and 7942-KU after a 2-week incubation in round bottom flasks under static conditions. Pictures represent a top view of the flask. (B) 24-h sedimentation assay (15 mL) in universal containers (30 mL) incubated under static conditions. (C) Biofilm determination in 7942-WT, 7942-KU, and 7942-WT Δ*pilB1* after a 5-day incubation in BG-11 medium. $n = 3$, error bars: standard deviation.

TABLE 1 7942-KU and 7942-AMC06 SNPs in protein-coding regions of the genome.

7942-WT locus	Locus description	7942-KU SNPs	7942-AMC06 SNPs (Adomako et al., 2022)
Synpcc7942_0095	Transcriptional regulator RpaA	Q121R	Q121R
Synpcc7942_0918	Long-chain acyl-CoA synthetase Aas	L295P	L295P
Synpcc7942_0918	Long-chain acyl-CoA synthetase Aas	T625I	T625I
Synpcc7942_1295	Acyltransferase	del TCATGCC	S305I
Synpcc7942_1510	Group 3 RNA polymerase sigma factor SigF	S239P	–
Synpcc7942_2070	Type IVa pilus retraction ATPase PilT1	C73Y	–
Synpcc7942_2373	L-alanine-DL-glutamate epimerase	G264D	G264V
Synpcc7942_2597	Adenylate cyclase	R89L	–

Overall, our findings support that 7942-KU has a fast sedimenting, but not biofilm-forming phenotype.

Unique mutations shed light on the history of *S. elongatus* PCC 7942-KU

Having observed that 7942-KU sediments significantly faster than 7942-WT, we aimed to determine the genetic differences that underlie this phenotype. 7942-KU was resequenced and, in comparison to the WT sequence (GenBank accession no. NC_007604), it has 8 SNPs in protein-coding regions (Table 1) and 95 SNPs in intergenic regions (Data S2). Of these 95, four were found within 500 bp upstream of regions coding for proteins Synpcc7942_0919, Synpcc7942_1296, Synpcc7942_1475, and Synpcc7942_2372. In addition, the 7942-KU genome was compared to the

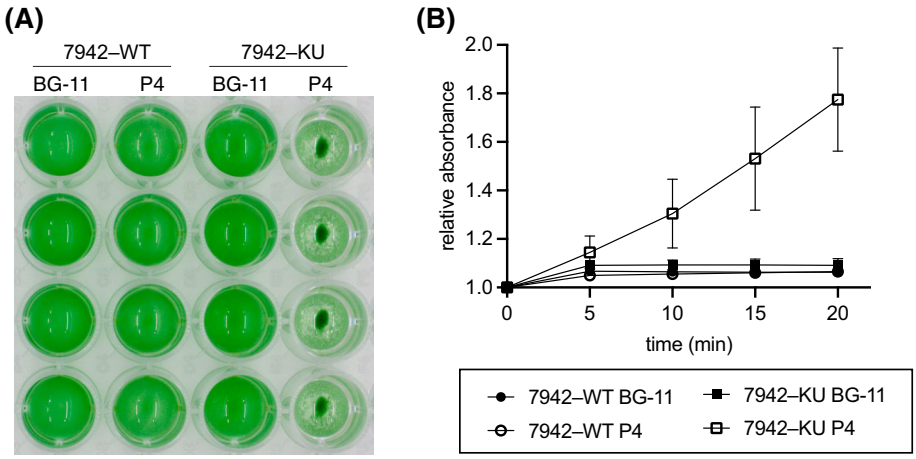

FIGURE 2 Development and testing of a high-throughput sedimentation assay. (A) Sedimentation of 7942-KU in a 48-well microplate after a 20 min static incubation. Four replicates of each sample are visible in the figure. (B) Microplate quantification of 7942-WT and 7942-KU sedimentation after cultivation in BG-11 and P4 media. $n = 4$, error bars: standard deviation.

recently published genome of *S. elongatus* PCC 7942-AMC06 (a strain routinely used in the laboratory of Susan Golden, UC San Diego) (Adomako et al., 2022). Out of the eight SNPs in protein-coding regions initially identified in 7942-KU, three also exist in 7942-AMC06, and another two are present in the same genes but encode different protein sequence variations (Table 1).

The three 7942-KU genes with unique SNPs are sigF (Synpcc7942_1510), pilT1 (Synpcc7942_2070), and an adenylate cyclase (Synpcc7942_2597). Given that a sedimentation phenotype has not been reported for 7942-AMC06, the following analysis focused on these three genes with unique mutations.

A novel microplate assay facilitates high-throughput quantitative analysis of sedimentation

The 24-h sedimentation assay in universal tubes (Figure 1B) is not quantitative and does not easily allow for multiple testing. Therefore, before proceeding with further analysis of the sedimentation phenotype, a miniaturized microplate-based sedimentation assay was developed. This assay relies on the observation that, in 48-well microplates, cells rapidly sedimented to the center of the well during static incubation (Figure 2A). A multipoint reading of the well absorbance then allowed for an estimation of the relative amount of biomass that has accumulated in a narrow area in the center of the well at each time point. This enabled the use of absorbance as a quantitative proxy for sedimentation. As a proof of concept, 7942-WT and 7942-KU were grown in BG-11 and P4 and multipoint absorbances were measured over a period of 20 min (Figure 2B). The accelerated sedimentation of 7942-KU was already visible at 5 min and continuously increased over the course of the measurement. Meanwhile, the sedimentation of the remaining strains was negligible throughout the whole period. The data from the microplate assay agreed with what was previously observed in the 24-h assay and offered a way to rapidly, and quantitatively, measure strain sedimentation.

Alterations in SigF and cell surface structures underpin fast sedimentation

Using the microplate-based sedimentation assay, we then proceeded to determine the individual effect of the three unique SNPs found in protein-coding regions (Synpcc7942_2070, Synpcc7942_2597, and Synpcc7942_1510). Synpcc7942_2070 encodes the T4aP retraction ATPase PilT1. Inactivation of PilT1 in *Synechocystis* leads to the display of an excessive amount of pili on the cell surface and an increase in cell aggregation (Bhaya et al., 2000; Conradi et al., 2019). To test whether hyperpiliation could contribute to the fast sedimentation phenotype, we constructed a PilT1 deletion mutant. No significant difference was observed in sedimentation between 7942-WT Δ*pilT1* and 7942-WT (Figure S3). The 7942-KU mutation present in the adenylate cyclase Synpcc7942_2597 affects the conserved arginine at position 89 which completely abolishes enzyme activity (Keppetipola et al., 2007). It has been shown that phenotypes derived from the lack of intracellular cAMP can be complemented by the addition of exogenous cAMP (Bhaya et al., 2006; Terauchi & Ohmori, 1999). Therefore, to determine if Synpcc7942_2597 could be responsible for the 7942-KU phenotype, cultures were grown in P4 medium, and the sedimentation assay was performed in the presence and absence of cAMP. No significant

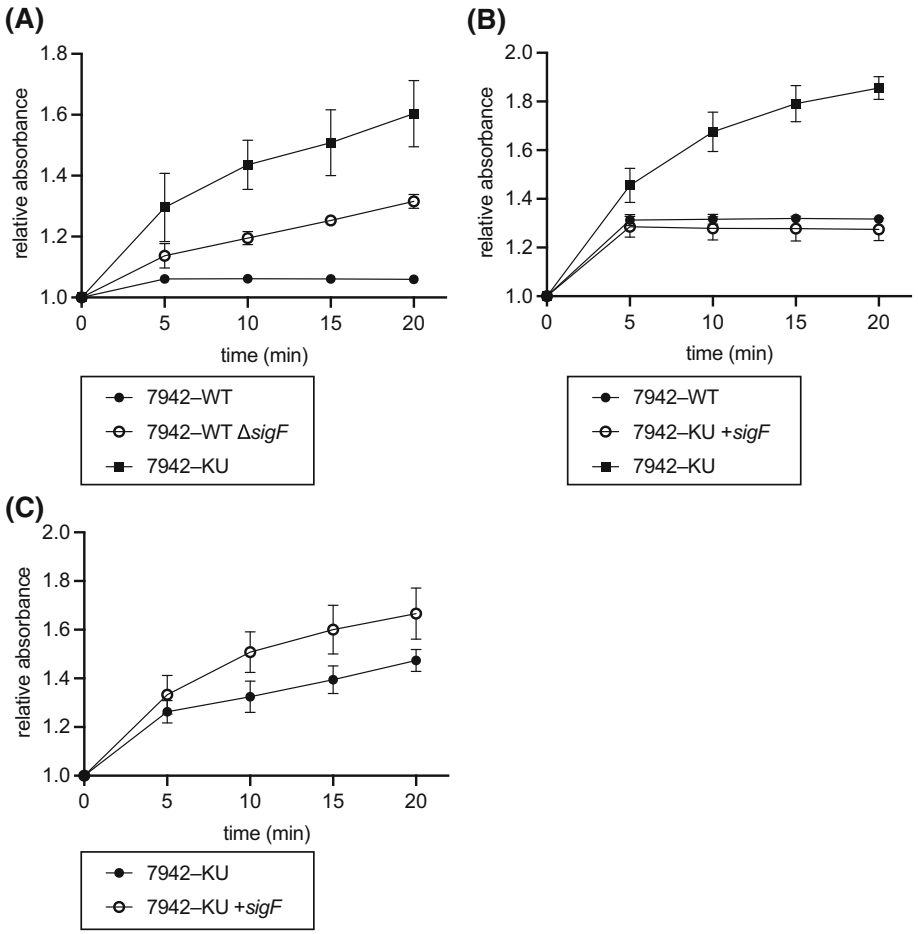

FIGURE 3 Sedimentation analysis of 7942-WT Δ*sigF* and 7942-KU + *sigF*. (A) Microplate quantification of 7942-WT, 7942-KU, and 7942-WT Δ*sigF* sedimentation after cultivation in P4 medium. $n = 4$, error bars: standard deviation. (B) Microplate quantification of 7942-WT, 7942-KU, and 7942-KU + *sigF* sedimentation after cultivation in BG-11 medium and addition of 100 mM NaCl. $n = 4$, error bars: standard deviation. (C) Microplate quantification of 7942-KU and 7942-KU + *sigF* sedimentation after cultivation in P4 medium. $n = 4$, error bars: standard deviation.

difference in sedimentation was observed (Figure S4). Having ruled out the effect of cAMP and hyperpiliation on the sedimentation phenotype, we proceeded to investigate the role of *sigF* (Synpcc7942_1510) in the fast sedimentation phenotype.

Synpcc7942_1510 encodes the Group 3 RNA polymerase sigma factor SigF. The S239P mutation eliminates one of the conserved amino acids required for DNA binding and recognition of the −35 promoter element (Bhaya et al., 1999). Therefore, a 7942-WT SigF knockout mutant was generated and the sedimentation rate of the 7942-WT Δ*sigF* mutant was measured (Figure 3A). The Δ*sigF* mutant sedimented significantly faster than its WT counterpart, albeit still slower than 7942-KU. We then proceeded to complement 7942-KU with the 7942-WT *sigF* gene variant and observed a partial complementation. In lower ionic strengths (i.e., 100 mM NaCl), cells sedimented at a similar rate to 7942-WT (Figure 3B). However, when grown in higher ionic strengths (i.e., P4 medium), the sedimentation rate of the complemented 7942-KU + *sigF* was similar to 7942-KU (Figure 3C). These results confirmed that SigF plays a key role in the fast sedimentation phenotype, however, it did not clarify the mechanism behind the fast sedimentation. In *Synechocystis*, SigF inactivation increases extracellular polymeric substances (EPS) and leads to changes in the cell surface composition which include the inactivation of T4aP (Bhaya et al., 1999; Flores et al., 2019). Therefore, to determine if the fast sedimentation phenotype of 7942-KU and 7942-WT Δ*sigF* was a result of alterations in polysaccharide release or cell surface composition, we took three approaches: measurement of the cell hydrophobicity, determination of EPS, and sedimentation analysis of an unpiliated mutant.

First, a MATH assay (Rosenberg, 1984; Rosenberg et al., 1980) was performed with 7942-WT, 7942-KU, and 7942-WT Δ*sigF*. This assay uses the level of bacterial adherence to an organic phase (typically an alkane) as a measure of the hydrophobicity of the cell surface. Typically, a less hydrophobic cell surface, or a cell surface that has lost hydrophobic structures such

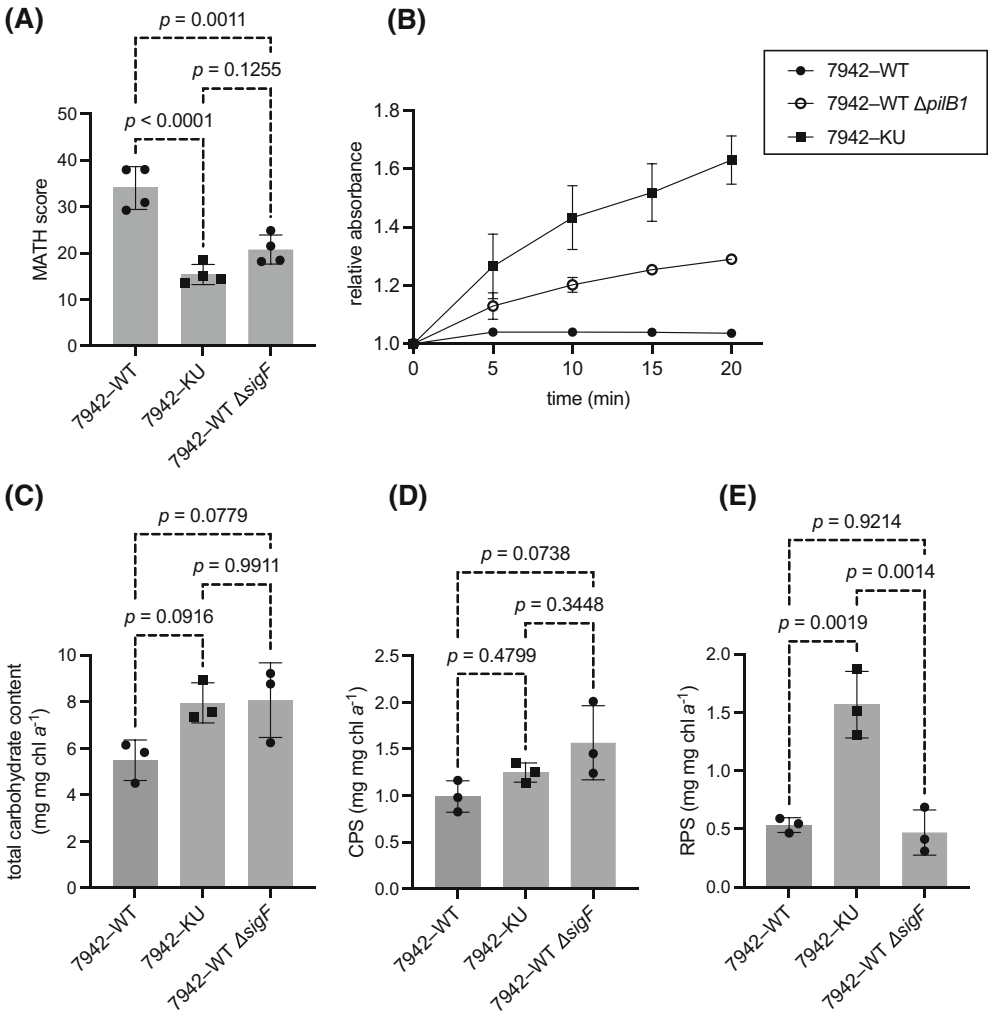

FIGURE 4 Cell surface hydrophobicity and EPS content of 7942-WT, 7942-KU, and 7942-WT Δ*sigF* and sedimentation analysis of 7942-WT Δ*pilB1*. (A) Surface hydrophobicity scores for 7942-WT, 7942-KU, and 7942-WT Δ*sigF*. The microbial adhesion to hydrocarbons (MATH) assay was performed with cells cultivated in P4 medium. $n = 4$, error bars: standard deviation. *P*-values were determined using a one-way ANOVA followed by a Tukey's multiple comparison test. (B) Microplate quantification of 7942-WT, 7942-KU, and 7942-WT Δ*pilB1* sedimentation after cultivation in P4 medium. $n = 4$, error bars: standard deviation. (C)–(E) Determination of EPS in 7942-WT, 7942-KU, and 7942-WT Δ*sigF*. Amount of total carbohydrate (C), capsular (D), and released (E) polysaccharides is shown. Cells were cultivated in P4 medium. $n = 3$, error bars: standard deviation. *P*-values were determined using a one-way ANOVA followed by a Tukey's multiple comparison test. CPS = capsular polysaccharides, RPS = released polysaccharides.

as flagella or pili, will result in a lower MATH score. We observed that both 7942-KU and 7942-WT Δ*sigF* had significantly less hydrophobic cell surfaces than 7942-WT (Figure 4A). Next, to determine if the lack of T4aP was a potential factor in the fast sedimentation phenotype, the sedimentation rate of the unpiliated 7942-WT Δ*pilB1* strain was measured. The results show that the strain sediments significantly faster than its WT counterpart and at virtually an identical rate to 7942-WT Δ*sigF* (Figure 4B). Finally, we proceeded to quantify EPS in the three strains (Figure 4C-E). The results showed that there was no significant difference in total carbohydrates (Figure 4C) or CPS (Figure 4D). However, interestingly, 7942-KU exhibited a 3-fold increase in RPS (Figure 4E). To confirm whether RPS were contributing to fast sedimentation we compared the sedimentation rates of 7942-KU before and after washing the cells with fresh medium. After washing, the sedimentation rate of 7942-KU was significantly lower than that of the original culture (Figure S5). Taken together, the data suggest a contribution of extracellular polysaccharides to the fast sedimentation phenotype. Taken together, these results suggest that differences in the cyanobacterial cell surface and amount of RPS account for the differential sedimentation observed between strains.

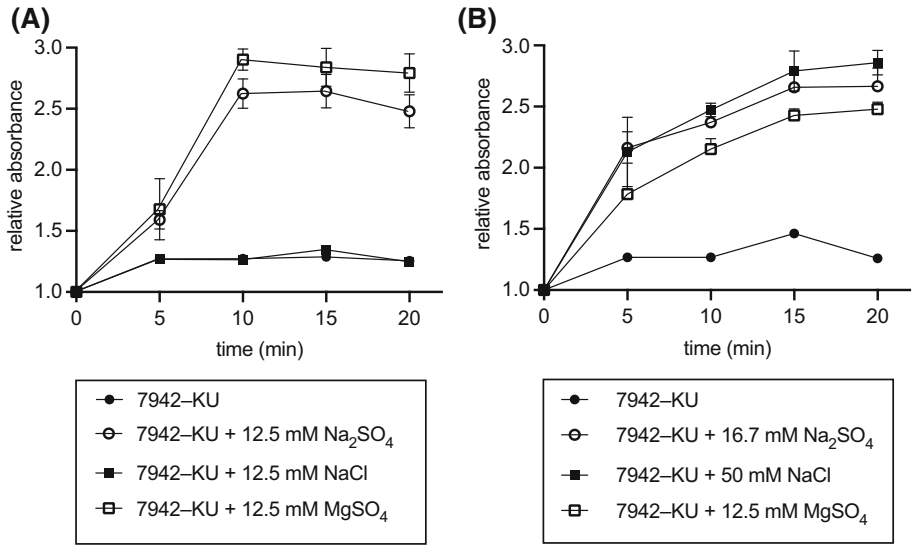

FIGURE 5 Microplate quantification of 7942-KU sedimentation after cultivation in BG-11 medium and addition of different salts. (A) 7942-KU sedimentation after addition of 12.5 mM of NaCl, Na_2SO_4, and $MgSO_4$. (B) 7942-KU sedimentation after addition of 50, 16.7, and 12.5 mM of NaCl, Na_2SO_4, and $MgSO_4$, respectively. $n = 4$, error bars: standard deviation.

Sedimentation is triggered by an increase in ionic strength of the medium

For biotechnological applications, it is important to determine the factors that induced accelerated sedimentation in P4 medium. Therefore, we started by comparing the components in BG-11 and P4 media (Table S3). One difference that stood out was that the concentration of $MgSO_4$ is almost seven times higher in P4 than in BG-11. $MgSO_4$ is a popular flocculant in several industries and it has previously been used for flocculation of algal cultures at high pH (Vandamme et al., 2012). To test the effect of $MgSO_4$ on sedimentation rates, 7942-KU was transferred to BG-11 medium with varying concentrations of the salt (0.3, 2, 4, and 8 mM) and then incubated in static conditions for 24 h (Figure S6). Sedimentation accelerated with increasing $MgSO_4$ concentrations with the fastest sedimentation being observed at 8 mM. This confirmed that $MgSO_4$ was influencing the sedimentation of the cultures, but the question remained whether this was due to a specific effect of the magnesium or sulphate ions or due to an increase in salt concentration. To answer this question, The microplate assay was then used to compare the effect of $MgSO_4$, Na_2SO_4, and NaCl supplementation on sedimentation rates.

For these experiments, 7942-WT and 7942-KU were grown in BG-11 medium to an exponential growth phase, then different salts were added to the cultures, and sedimentation was measured after 2 h. When the salts were added in the same concentration (12.5 mM), $MgSO_4$ and Na_2SO_4 induced sedimentation, however, there was no significant difference between the addition of NaCl and the control (Figure 5A). Considering the ionic strengths, 12.5 mM solutions of $MgSO_4$, Na_2SO_4, and NaCl have ionic strengths of 50, 37.5, and 12.5 mM, respectively. Therefore, we tested adding the different salts in different concentrations to achieve the same ionic strength of 50 mM across all salts tested (Figure 5B). In this case, we observed sedimentation in all three salt treatments with no significant difference between them. In conclusion, the data support the hypothesis that an increase in ionic strength accelerates sedimentation. Going forward, this can be exploited as a strategy to improve biomass recovery at scale.

DISCUSSION

In this study, we describe 7942-KU, a novel *S. elongatus* substrain that, through the process of laboratory domestication, has acquired a fast-sedimenting phenotype. We further demonstrate that the accelerated sedimentation is mediated by interactions between higher ionic strengths, released polysaccharides, and altered cell surface characteristics. Laboratory domestication is typically an undesired outcome of serial culturing. However, here we show that a detailed characterization of domesticated cyanobacterial strains can provide insights into key cellular processes and open new perspectives for the biotechnological application of cyanobacteria.

Fast sedimenting strains are valuable for algal biotechnology

During microalgal production, harvesting can account for up to 30% of the total costs (Barros et al., 2015).

Therefore, there is a keen interest in developing low-cost harvesting processes. Harvesting typically consists of a two-step process where cultures are concentrated by flocculation/sedimentation prior to employing higher-cost physical cell separation techniques such as centrifugation or filtration. Many methods for large-scale cell concentration have been proposed, however, they typically involve the addition of a flocculating agent or the application of an electric field (Barros et al., 2015). In the case of 7942-KU, full sedimentation can be achieved quickly (< 12 h) without the addition of flocculating agents (Figure 1), thus allowing for easy product harvesting and recycling of the culture medium. In recent years, there have been several efforts to develop cyanobacterial strains with accelerated sedimentation rates. Strategies have generally focused on engineering cell size or, more commonly, cell surface/extracellular properties. An example of the former is a study that achieved accelerated sedimentation (48–72 h) by modifying the levels of Min system proteins in 7942-WT to obtain cells of near-millimetre lengths (Jordan et al., 2017). Regarding the manipulation of the cell surface, several approaches have resulted in fast-sedimenting cyanobacterial strains. These include inactivation of O-antigen synthesis (Simkovsky et al., 2012), manipulation of the amount/composition of EPS (Flores et al., 2019; Jittawuttipoka et al., 2013; Li et al., 2021), T4aP modification (Allen et al., 2019; Conradi et al., 2019; Nagar et al., 2017) and the secretion of a hydrophobic product (e.g., limonene) (Long et al., 2022). Our data suggest that the best approach to improving biomass recovery will be multi-layered, potentially combining engineering of cell size, cell surface, and EPS with a medium optimized to induce fast sedimentation.

The cyanobacterial cell surface plays a significant role in the transition from a planktonic to a benthic state

The properties of the cyanobacterial cell surface have repeatedly been associated with regulating repulsion or attraction of cells. The mechanisms vary but typically include changes in cell surface structures (e.g., pili and S-layer), EPS, vesiculation, and the composition of the extracellular matrix (Allen et al., 2019; Conradi et al., 2019; Flores et al., 2019; Kera et al., 2020; Schatz et al., 2013). In agreement with this, our findings suggest the 7942-KU fast sedimentation phenotype is caused by a combination of altered cell surface and an increase in RPS. Cell surface modifications can increase the exposure of the cell to environmental fluctuations, thus leading to the observed fast sedimentation under higher ionic strengths. In the MATH assay, 7942-KU and 7942-WT Δ*sigF* showed significantly lower cell surface hydrophobicities (Figure 4A). In heterotrophic bacteria, a lower MATH score has been associated with higher sedimentation rates due to the loss or alteration of a diversity of surface structures such as lipopolysaccharides, flagella, the S-layer, or T4aP (Lahesaare et al., 2016; Martínez-García et al., 2020; van der Mei et al., 2003). Given that 7942-WT Δ*sigF* and the unpiliated 7942-WT Δ*pilB1* also show accelerated sedimentation, we can hypothesize that a large part of the fast sedimentation in 7942-KU can be traced back to deregulation of SigF and alterations of cell surface composition. This is also consistent with the findings in *Synechocystis*, where the deletion of SigF dramatically changes the cyanobacterial extracellular milieu and also leads to fast sedimentation (Bhaya et al., 1999; Flores et al., 2019).

However, the inactivation of SigF did not completely account for the level of sedimentation observed in 7942-KU. Several studies have shown that modulating the amount and composition of EPS can drastically impact the repulsive forces between cells and their environment and lead to sedimentation (Allen et al., 2019; Conradi et al., 2019; Li et al., 2021). Accordingly, our data showed that 7942-KU releases approximately three-fold more polysaccharides in comparison to both 7942-WT and 7942-WT Δ*sigF*. Therefore, our data support the conclusion that RPS play a role in the 7942-KU fast sedimentation phenotype in addition to the cell surface alterations originating from disruption of SigF. SNPs in regions coding for proteins involved in exopolysaccharide synthesis or release were, however, not identified in the 7942–KU genome. Therefore, further investigation is required.

CONCLUDING REMARKS

Laboratory domestication is a global phenomenon and virtually all model organisms have undergone this process. However, the impact of domestication on research outcomes is still underestimated. Going forward, it is important that genomic differences among substrains be considered during experimental planning. In addition, a detailed investigation of domesticated substrains can help to elucidate how cyanobacteria adapt to a changing environment.

AUTHOR CONTRIBUTIONS

Julie A. Z. Zedler: Data curation (equal); formal analysis (equal); investigation (equal); methodology (equal); resources (equal); visualization (equal); writing – original draft (equal); writing – review and editing (equal). **Marlene Michel:** Data curation (equal); formal analysis (equal); investigation (equal); methodology (equal); visualization (equal); writing – review and editing (equal). **Georg Pohnert:** Resources (equal); writing – review and editing (equal). **David A. Russo:** Conceptualization (equal); data curation (equal); formal analysis (equal); funding

acquisition (equal); investigation (equal); methodology (equal); resources (equal); writing – original draft (equal); writing – review and editing (equal).

ACKNOWLEDGEMENTS

The authors thank Yumiko Sakuragi for providing the *S. elongatus* PCC 7942-KU strain.

DAR was supported by the Alexander von Humboldt Foundation and by the IMPULSE project (IP-2020-03, Friedrich Schiller University Jena). This work was funded by the Deutsche Forschungsgemeinschaft (DFG, German Research Foundation) under Germany's Excellence Strategy—EXC 2051—Project-ID 390713860 (JAZZ) and by the Deutsche Forschungsgemeinschaft (DFG, German Research Foundation), SFB 1127 ChemBioSys, project number 239748522 (JAZZ). Open Access funding enabled and organized by Projekt DEAL.

CONFLICT OF INTEREST STATEMENT

The authors declare no conflict of interest.

DATA AVAILABILITY STATEMENT

Raw read files and variant analysis from the Eurofins Genomics resequencing of PCC 7942-KU and plasmid maps for pJZ170, pMM002, pDAR27 and can be found at 10.5281/zenodo.7299545. PCC 7942-KU is available from the DSMZ—German Collection of Microorganisms and Cell Cultures (DSM no. 115314).

ORCID

Julie A. Z. Zedler https://orcid.org/0000-0002-0462-8810
Georg Pohnert https://orcid.org/0000-0003-2351-6336
David A. Russo https://orcid.org/0000-0002-4729-1701

REFERENCES

Adomako, M., Ernst, D., Simkovsky, R., Chao, Y.-Y., Wang, J., Fang, M. et al. (2022) Comparative genomics of *Synechococcus elongatus* explains the phenotypic diversity of the strains. *MBio*, 13, e0086222.

Allen, R., Rittmann, B.E. & Curtiss, R. (2019) Axenic biofilm formation and aggregation by *Synechocystis* sp. strain PCC 6803 are induced by changes in nutrient concentration and require cell surface structures. *Applied and Environmental Microbiology*, 85, e02192-18.

Barros, A.I., Gonçalves, A.L., Simões, M. & Pires, J.C.M. (2015) Harvesting techniques applied to microalgae: a review. *Renewable and Sustainable Energy Reviews*, 41, 1489–1500.

Bhaya, D., Bianco, N.R., Bryant, D. & Grossman, A. (2000) Type IV pilus biogenesis and motility in the cyanobacterium *Synechocystis* sp. PCC 6803. *Molecular Microbiology*, 37, 941–951.

Bhaya, D., Nakasugi, K., Fazeli, F. & Burriesci, M.S. (2006) Phototaxis and impaired motility in adenylyl cyclase and cyclase receptor protein mutants of *Synechocystis* sp. strain PCC 6803. *Journal of Bacteriology*, 188, 7306–7310.

Bhaya, D., Watanabe, N., Ogawa, T. & Grossman, A.R. (1999) The role of an alternative sigma factor in motility and pilus formation in the cyanobacterium *Synechocystis* sp. strain PCC6803. *Proceedings of the National Academy of Sciences of the United States of America*, 96, 3188–3193.

Bryant, D.A. (2014) A brief history of cyanobacterial research: past, present, and future prospects. In: *The cell biology of cyanobacteria*. Poole, UK: Caister Academic Press, pp. 1–5.

Cao, J., Russo, D.A., Xie, T., Groß, G.A. & Zedler, J.A.Z. (2022) A droplet-based microfluidic platform enables high-throughput combinatorial optimization of cyanobacterial cultivation. *Scientific Reports*, 12, 15536.

Cohen, S.E. & Golden, S.S. (2015) Circadian rhythms in cyanobacteria. *Microbiology and Molecular Biology Reviews*, 79, 373–385.

Conradi, F.D., Zhou, R.-Q., Oeser, S., Schuergers, N., Wilde, A. & Mullineaux, C.W. (2019) Factors controlling floc formation and structure in the cyanobacterium *Synechocystis* sp. strain PCC 6803. *Journal of Bacteriology*, 201, e00344-19.

DuBois, M., Gilles, K.A., Hamilton, J.K., Rebers, P.A. & Smith, F. (1956) Colorimetric method for determination of sugars and related substances. *Analytical Chemistry*, 28, 350–356.

Eydallin, G., Ryall, B., Maharjan, R. & Ferenci, T. (2014) The nature of laboratory domestication changes in freshly isolated *Escherichia coli* strains. *Environmental Microbiology*, 16, 813–828.

Flores, C., Santos, M., Pereira, S.B., Mota, R., Rossi, F., de Philippis, R. et al. (2019) The alternative sigma factor SigF is a key player in the control of secretion mechanisms in *Synechocystis* sp. PCC 6803. *Environmental Microbiology*, 21, 343–359.

Gibson, D.G., Young, L., Chuang, R.-Y., Venter, J.C., Hutchison, C.A. & Smith, H.O. (2009) Enzymatic assembly of DNA molecules up to several hundred kilobases. *Nature Methods*, 6, 343–345.

Golden, S.S. (2019) The international journeys and aliases of *Synechococcus elongatus*. *New Zealand Journal of Botany*, 57, 70–75.

Ikeuchi, M. & Tabata, S. (2001) *Synechocystis* sp. PCC 6803—a useful tool in the study of the genetics of cyanobacteria. *Photosynthesis Research*, 70, 73–83.

Jittawuttipoka, T., Planchon, M., Spalla, O., Benzerara, K., Guyot, F., Cassier-Chauvat, C. et al. (2013) Multidisciplinary evidences that *Synechocystis* PCC6803 exopolysaccharides operate in cell sedimentation and protection against salt and metal stresses. *PLoS One*, 8, e55564.

Jordan, A., Chandler, J., MacCready, J.S., Huang, J., Osteryoung, K.W. & Ducat, D.C. (2017) Engineering cyanobacterial cell morphology for enhanced recovery and processing of biomass. *Applied and Environmental Microbiology*, 83, e00053-17.

Kaneko, T., Sato, S., Kotani, H., Tanaka, A., Asamizu, E., Nakamura, Y. et al. (1996) Sequence analysis of the genome of the unicellular cyanobacterium *Synechocystis* sp. strain PCC6803. II. Sequence determination of the entire genome and assignment of potential protein-coding regions. *DNA Research*, 3, 109–136.

Keppetipola, N., Jain, R. & Shuman, S. (2007) Novel triphosphate phosphohydrolase activity of clostridium thermocellum TTM, a member of the triphosphate tunnel metalloenzyme superfamily*. *The Journal of Biological Chemistry*, 282, 11941–11949.

Kera, K., Yoshizawa, Y., Shigehara, T., Nagayama, T., Tsujii, M., Tochigi, S. et al. (2020) Hik36–Hik43 and Rre6 act as a two-component regulatory system to control cell aggregation in *Synechocystis* sp. PCC6803. *Scientific Reports*, 10, 19405.

Lahesaare, A., Ainelo, H., Teppo, A., Kivisaar, M., Heipieper, H.J. & Teras, R. (2016) LapF and its regulation by Fis affect the cell surface hydrophobicity of pseudomonas putida. *PLoS One*, 11, e0166078.

Li, J., Fang, D., Ye, R., Zhou, C. & Li, P. (2021) The released polysaccharide inhibits cell aggregation and biofilm formation in the

cyanobacterium *Synechocystis* sp. PCC 6803. *European Journal of Phycology*, 56, 119–128.
Li, S., Sun, T., Xu, C., Chen, L. & Zhang, W. (2018) Development and optimization of genetic toolboxes for a fast-growing cyanobacterium *Synechococcus elongatus* UTEX 2973. *Metabolic Engineering*, 48, 163–174.
Lippi, L., Bähr, L., Wüstenberg, A., Wilde, A. & Steuer, R. (2018) Exploring the potential of high-density cultivation of cyanobacteria for the production of cyanophycin. *Algal Research*, 31, 363–366.
Long, B., Fischer, B., Zeng, Y., Amerigian, Z., Li, Q., Bryant, H. et al. (2022) Machine learning-informed and synthetic biology-enabled semi-continuous algal cultivation to unleash renewable fuel productivity. *Nature Communications*, 13, 541.
Martínez-García, E., Fraile, S., Rodríguez Espeso, D., Vecchietti, D., Bertoni, G. & de Lorenzo, V. (2020) Naked bacterium: emerging properties of a surfome-streamlined *Pseudomonas putida* strain. *ACS Synthetic Biology*, 9, 2477–2492.
Mota, R., Guimarães, R., Büttel, Z., Rossi, F., Colica, G., Silva, C.J. et al. (2013) Production and characterization of extracellular carbohydrate polymer from *Cyanothece* sp. CCY 0110. *Carbohydrate Polymers*, 92, 1408–1415.
Nagar, E., Zilberman, S., Sendersky, E., Simkovsky, R., Shimoni, E., Gershtein, D. et al. (2017) Type 4 pili are dispensable for biofilm development in the cyanobacterium *Synechococcus elongatus*. *Environmental Microbiology*, 19, 2862–2872.
Ritchie, R.J. (2008) Universal chlorophyll equations for estimating chlorophylls a, b, c, and d and total chlorophylls in natural assemblages of photosynthetic organisms using acetone, methanol, or ethanol solvents. *Photosynthetica*, 46, 115–126.
Rosenberg, M. (1984) Ammonium sulphate enhances adherence of *Escherichia coli* J-5 to hydrocarbon and polystyrene. *FEMS Microbiology Letters*, 25, 41–45.
Rosenberg, M., Gutnick, D. & Rosenberg, E. (1980) Adherence of bacteria to hydrocarbons: a simple method for measuring cell-surface hydrophobicity. *FEMS Microbiology Letters*, 9, 29–33.
Russo, D.A., Zedler, J.A.Z., Conradi, F.D., Schuergers, N., Jensen, P.E., Mullineaux, C.W. et al. (2022) Development of a highly sensitive luciferase-based reporter system to study two-step protein secretion in cyanobacteria. *Journal of Bacteriology*, 204, e00504–e00521.
Russo, D.A., Zedler, J.A.Z., Wittmann, D.N., Möllers, B., Singh, R.K., Batth, T.S. et al. (2019) Expression and secretion of a lytic polysaccharide monooxygenase by a fast-growing cyanobacterium. *Biotechnology for Biofuels*, 12, 74.
Santos-Merino, M., Singh, A.K. & Ducat, D.C. (2019) New applications of synthetic biology tools for cyanobacterial metabolic engineering. *Frontiers in Bioengineering and Biotechnology*, 7, 1–24.
Schatz, D., Nagar, E., Sendersky, E., Parnasa, R., Zilberman, S., Carmeli, S. et al. (2013) Self-suppression of biofilm formation in the cyanobacterium *Synechococcus elongatus*. *Environmental Microbiology*, 15, 1786–1794.
Schirmacher, A.M., Hanamghar, S.S. & Zedler, J.A.Z. (2020) Function and benefits of natural competence in cyanobacteria: from ecology to targeted manipulation. *Life*, 10, 249.
Schuergers, N., Lenn, T., Kampmann, R., Meissner, M.V., Esteves, T., Temerinac-Ott, M. et al. (2016) Cyanobacteria use micro-optics to sense light direction. *eLife*, 5, e12620.
Sendersky, E., Simkovsky, R., Golden, S. & Schwarz, R. (2017) Quantification of chlorophyll as a proxy for biofilm formation in the cyanobacterium *Synechococcus elongatus*. *Bio-Protocol*, 7, e2406.
Simkovsky, R., Daniels, E.F., Tang, K., Huynh, S.C., Golden, S.S. & Brahamsha, B. (2012) Impairment of O-antigen production confers resistance to grazing in a model amoeba–cyanobacterium predator–prey system. *Proceedings of the National Academy of Sciences of the United States of America*, 109, 16678–16683.
Stanier, R.Y., Kunisawa, R., Mandel, M. & Cohen-Bazire, G. (1971) Purification and properties of unicellular blue-green algae (order Chroococcales). *Bacteriological Reviews*, 35, 171–205.
Taton, A., Erikson, C., Yang, Y., Rubin, B.E., Rifkin, S.A., Golden, J.W. et al. (2020) The circadian clock and darkness control natural competence in cyanobacteria. *Nature Communications*, 11, 1688.
Terauchi, K. & Ohmori, M. (1999) An adenylate cyclase, cyal, regulates cell motility in the cyanobacterium *Synechocystis* sp. PCC 6803. *Plant & Cell Physiology*, 40, 248–251.
Trautmann, D., Voß, B., Wilde, A., Al-Babili, S. & Hess, W.R. (2012) Microevolution in cyanobacteria: Re-sequencing a motile substrain of *Synechocystis* sp. PCC 6803. *DNA Research*, 19, 435–448.
Ungerer, J., Lin, P.-C., Chen, H.-Y. & Pakrasi, H.B. (2018) Adjustments to photosystem stoichiometry and electron transfer proteins are key to the remarkably fast growth of the cyanobacterium *Synechococcus elongatus* UTEX 2973. *MBio*, 9, e02327-17.
Ungerer, J., Wendt, K.E., Hendry, J.I., Maranas, C.D. & Pakrasi, H.B. (2018) Comparative genomics reveals the molecular determinants of rapid growth of the cyanobacterium *Synechococcus elongatus* UTEX 2973. *Proceedings of the National Academy of Sciences of the United States of America*, 115, E11761–E11770.
van der Mei, H.C., van de Belt-Gritter, B., Pouwels, P.H., Martinez, B. & Busscher, H.J. (2003) Cell surface hydrophobicity is conveyed by S-layer proteins—a study in recombinant lactobacilli. *Colloids and Surfaces, B: Biointerfaces*, 28, 127–134.
Vandamme, D., Foubert, I., Fraeye, I., Meesschaert, B. & Muylaert, K. (2012) Flocculation of Chlorella vulgaris induced by high pH: role of magnesium and calcium and practical implications. *Bioresource Technology*, 105, 114–119.
Vasudevan, R., Gale, G.A.R., Schiavon, A.A., Puzorjov, A., Malin, J., Gillespie, M.D. et al. (2019) CyanoGate: a modular cloning suite for engineering cyanobacteria based on the plant MoClo syntax. *Plant Physiology*, 180, 39–55.
Williams, J.G.K. (1988) [85] Construction of specific mutations in photosystem II photosynthetic reaction center by genetic engineering methods in *Synechocystis* 6803. In: *Methods in enzymology* Cyanobacteria. San Diego, CA: Academic Press, pp. 766–778.
Yang, Y., Lam, V., Adomako, M., Simkovsky, R., Jakob, A., Rockwell, N.C. et al. (2018) Phototaxis in a wild isolate of the cyanobacterium *Synechococcus elongatus*. *Proceedings of the National Academy of Sciences of the United States of America*, 115, E12378–E12387.
Yu, J., Liberton, M., Cliften, P.F., Head, R.D., Jacobs, J.M., Smith, R.D. et al. (2015) *Synechococcus elongatus* UTEX 2973, a fast growing cyanobacterial chassis for biosynthesis using light and CO_2. *Scientific Reports*, 5, 8132.

SUPPORTING INFORMATION

Additional supporting information can be found online in the Supporting Information section at the end of this article.

How to cite this article: Zedler, J.A.Z., Michel, M., Pohnert, G. & Russo, D.A. (2023) Cell surface composition, released polysaccharides, and ionic strength mediate fast sedimentation in the cyanobacterium *Synechococcus elongatus* PCC 7942. *Environmental Microbiology*, 25(10), 1955–1966. Available from: https://doi.org/10.1111/1462-2920.16426